

Intrinsic dynamics of an enzyme underlies catalysis

Elan Z. Eisenmesser¹, Oscar Millet^{2†}, Vladimir Labeikovsky¹, Dmitry M. Korzhnev², Magnus Wolf-Watz^{1†}, Daryl A. Bosco^{1†}, Jack J. Skalicky^{3†}, Lewis E. Kay² & Dorothee Kern¹

A unique feature of chemical catalysis mediated by enzymes is that the catalytically reactive atoms are embedded within a folded protein. Although current understanding of enzyme function has been focused on the chemical reactions and static three-dimensional structures, the dynamic nature of proteins has been proposed to have a function in catalysis^{1–5}. The concept of conformational substates has been described⁶; however, the challenge is to unravel the intimate linkage between protein flexibility and enzymatic function. Here we show that the intrinsic plasticity of the protein is a key characteristic of catalysis. The dynamics of the prolyl *cis*–*trans* isomerase cyclophilin A (CypA) in its substrate-free state and during catalysis were characterized with NMR relaxation experiments. The characteristic enzyme motions detected during catalysis are already present in the free enzyme with frequencies corresponding to the catalytic turnover rates. This correlation suggests that the protein motions necessary for catalysis are an intrinsic property of the enzyme and may even limit the overall turnover rate. Motion is localized not only to the active site but also to a wider dynamic network. Whereas coupled networks in proteins have been proposed previously^{3,7–10}, we experimentally measured the collective nature of motions with the use of mutant forms of CypA. We propose that the pre-existence of collective dynamics in enzymes before catalysis is a common feature of biocatalysts and that proteins have evolved under synergistic pressure between structure and dynamics.

The most basic principle of enzyme catalysis is the ability of an enzyme to decrease the transition-state energy, thereby catalysing the chemical reaction. A wealth of information about the kinetics and thermodynamics of enzyme-catalysed reactions has been obtained by monitoring the conversion of substrates into products. However, much less is known about the kinetics and energetics of conformational processes in the protein. Because it is the protein component that alters the transition state energy, enzyme function depends on transitions from ground states to higher-energy states of the enzyme and the reactant. A detailed understanding of the entire trajectory of catalysis is therefore a current challenge. Structures of intermediates provide snapshots of conformational changes, and a set of experimental methods, such as fluorescence, mass spectroscopy and NMR, have been developed to monitor the kinetics of these changes. We have recently provided a proof of principle that enzyme dynamics can be monitored during catalysis at multiple sites by NMR relaxation experiments with the use of cyclophilin A (CypA)⁵. This enzyme belongs to the family of prolyl-isomerases that catalyse the *cis*–*trans* isomerization of prolyl peptide bonds. Although CypA is involved in a series of biomedically important processes¹¹, its natural biological role and mechanism of action are still in debate. CypA is the target of the

immunosuppressive drug cyclosporin A (CsA) and is essential for HIV-1 virulence¹².

Here we use new NMR relaxation dispersion experiments¹³ to compare motions in free CypA with those during turnover. We show that protein dynamics associated with catalysis is a built-in property of the enzyme that is also manifested in the free protein. The motions are collective, propagating from the active site to remote sites. The results show that intrinsic plasticity on a basic structural template is a crucial element for catalytic function, and that proteins have therefore evolved under synergistic pressure between structure and dynamics.

Relaxation dispersion experiments probe molecular motions in the microsecond to millisecond timescale quantitatively and with much higher sensitivity than traditional transverse relaxation experiments¹³. The additional line-broadening of NMR signals caused by conformational exchange between two states (R_{ex}) depends on the sum of forward and reverse rates of interconversion (k_{ex}), the relative populations of the exchanging species (p_A and p_B) and the chemical shifts between the exchanging species ($\Delta\omega$), with

$$R_{\text{ex}} = p_A p_B \frac{\Delta\omega^2}{k_{\text{ex}}} \left(1 - \frac{4\nu_{\text{CPMG}}}{k_{\text{ex}}} \tanh \frac{k_{\text{ex}}}{4\nu_{\text{CPMG}}} \right) \quad (1)$$

in the fast exchange limit¹⁴.

The dependence of R_{ex} on the applied external field (ν_{CPMG} , in which CPMG stands for Carr–Purcell–Meiboom–Gill) is the key element in relaxation dispersion experiments (Fig. 1a, b). It is noted that an atom with R_{ex} contributions reports on a change in its electronic environment, but this does not necessarily represent physical movement of this atom.

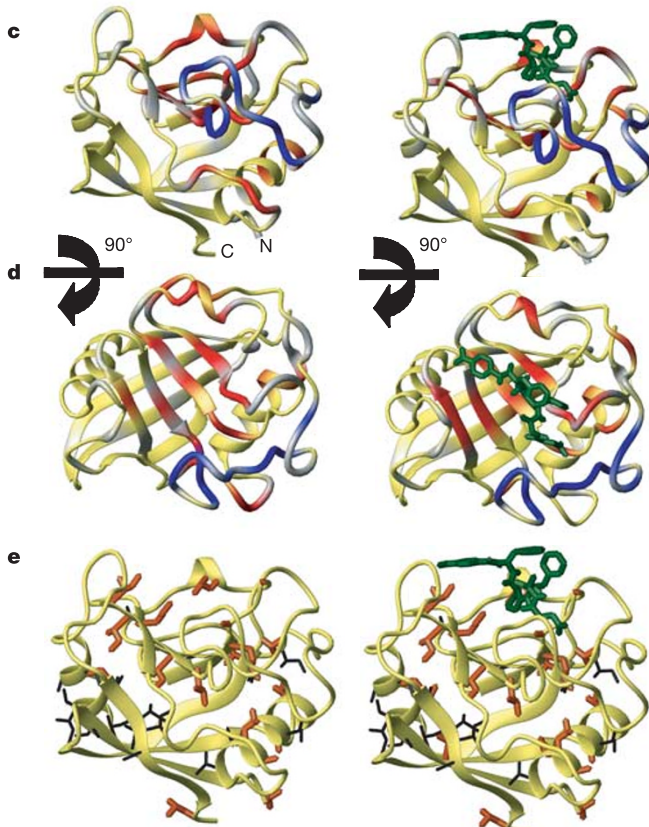
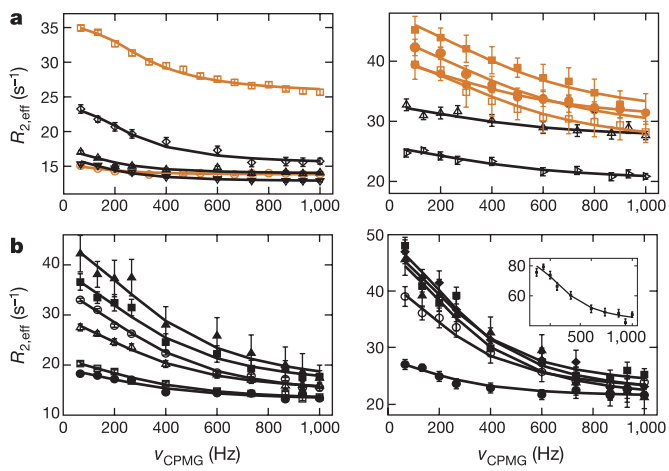
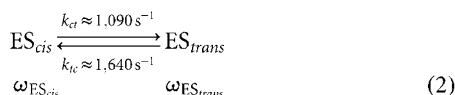
We applied this method to ¹⁵N-labelled CypA catalysing the *cis*–*trans* isomerization of *N*-succinyl-Ala-Phe-Pro-Phe-*p*-nitroanilide (Fig. 1, right). The high sensitivity of these experiments leads to the identification of many more amides in CypA with conformational exchange than originally described⁵. Clear and quantitative analysis of the relaxation data require conditions of two-state exchange. However, CypA interconverts between at least three states during the catalytic cycle: the free enzyme (E) and the two enzyme–substrate (ES) complexes with substrate bound in the *cis* and *trans* conformations. The system was therefore biochemically ‘tuned’ to two-state exchange: by using an excess of substrate at 10 °C, 95% saturation with substrate could be reached in which the dispersion profiles detect only two-state conformational exchange corresponding to the catalytic step of *cis*–*trans* isomerization (scheme (2)). Under these conditions, contributions to R_{ex} from substrate binding and dissociation are negligible (see Supplementary Information).

Individual fits of dispersion profiles on a collection of 30 amides resulted in similar rate constants, a remarkable result that justifies a

¹Department of Biochemistry, Howard Hughes Medical Institute, Brandeis University, Waltham, Massachusetts 02454, USA. ²Departments of Medical Genetics, Biochemistry and Chemistry, University of Toronto, Toronto, Ontario M5S 1A8, Canada. ³National High Magnetic Field Laboratory at Florida State University, Tallahassee, Florida 32310, USA.

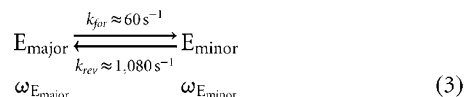
†Present addresses: Plataforma de Biomoléculas, Parc Científic de Barcelona, Josep Samitier 1–5, 08028 Barcelona, Catalonia, Spain (O.M.); The Scripps Research Institute, Department of Chemistry, La Jolla, California 92037, USA (D.A.B.); University of Utah School of Medicine, Department of Biochemistry, Salt Lake City, Utah 84132, USA (J.S.); University of Umeå, Department of Biochemistry, Umeå SE-901 87, Sweden (M.W.W.).

global fit with a single rate constant, k_{ex} (Fig. 1a, b, right). This result is further buttressed by ^{13}C -CPMG dispersion experiments on methyl side chains¹³ (Fig. 1a, right). Comparison of the dynamic hotspots of amide nitrogens (Fig. 1c, d) and methyl carbons (Fig. 1e) reveals an extended dynamic network emanating from the active site of CypA. ^{15}N and ^{13}C relaxation data could be globally fitted with the same k_{ex} value of $2,730 \pm 220 \text{ s}^{-1}$ (mean \pm s.d.) and separation into the individual rate constants (scheme (2)) was based on the relative populations of *cis* and *trans* bound substrates determined previously¹⁵. This k_{ex} value of protein motion is very close to the sum of the rate constants of *cis*-to-*trans* (k_{ct}) and *trans*-to-*cis* (k_{tc}) substrate isomerization on the enzyme ($k_{\text{ex}} = 2,500 \pm 500 \text{ s}^{-1}$; mean \pm s.d.)¹⁵.



Our earlier work indicated a possible intimate correlation between motion on the enzyme and substrate turnover⁵, but the system was underdetermined with respect to the exact rate of conformational exchange. The present results show explicitly that conformational changes of the enzyme coincide with substrate turnover.

Although it is not surprising that conformational rearrangements occur in the working enzyme, we found that most of these same residues exhibit exchange in the resting, substrate-free state (Fig. 1, left). Quantitative analysis revealed that most residues can be globally fitted with a k_{ex} value of $1,140 \pm 200 \text{ s}^{-1}$ (mean \pm s.d.) (Fig. 1a, left) for an exchange process between a major and a minor population (of less than 10%; see Methods). Notably, one of the exchange rates in free CypA is comparable to those observed during turnover:



It is also noteworthy that the calculated chemical-shift differences (equation (1)) between E_{major} and E_{minor} ($\omega_{\text{E}_{\text{major}}} - \omega_{\text{E}_{\text{minor}}}$; scheme (3)) are similar to those between ES_{cis} and ES_{trans} ($\omega_{\text{ES}_{\text{cis}}} - \omega_{\text{ES}_{\text{trans}}}$; scheme (2)) for residues remote from the substrate, suggesting that the *cis* substrate binds E_{major} to form ES_{cis} , whereas the *trans* substrate binds E_{minor} to form ES_{trans} . This would imply that binding of the substrates shifts the pre-existing, highly skewed equilibrium to a more balanced one.

Besides the interconversion detected between E_{major} and E_{minor} a specific region (the loop comprising residues 65–84) clearly moves faster, with a k_{ex} of $2,260 \pm 200 \text{ s}^{-1}$ (mean \pm s.d.) (Fig. 1b, left) in the free enzyme. This result implies that motions in proteins are usually more complex than mere interconversion between two conformational states. Folded proteins must in fact be described with a multidimensional energy landscape. However, with substrate bound, this loop seems to fluctuate collectively with the rest of the protein as catalysis occurs.

The fact that in free CypA all residues within the two groups can be

Figure 1 | Protein dynamics necessary for catalysis is an intrinsic property of the enzyme. Quantitative analysis of protein dynamics of resting (left) and working (right) CypA. **a, b**, Global fits of NMR relaxation dispersion data³⁰ using both ^{15}N backbone amide (black) and ^{13}C methyl groups (orange) of CypA in the absence of substrate (left) and during turnover (right) are shown. Residues in free CypA had to be globally fitted in two groups with $k_{\text{ex}} = 1,140 \pm 200 \text{ s}^{-1}$ for group I (**a**) and $k_{\text{ex}} = 2,260 \pm 200 \text{ s}^{-1}$ (means \pm s.d.) for group II (**b**), whereas during turnover the distinction of rates was not apparent and consequently all residues were globally fitted together with $k_{\text{ex}} = 2,730 \pm 220 \text{ s}^{-1}$ (mean \pm s.d.) (**a, b**, right panel). Residues $\text{Leu}^{39}\text{C}\delta 1$ (open square), $\text{Arg}^{55}\text{N}^{\text{H}}$ (open triangles, point sideways), $\text{Ile}^{57}\text{C}\gamma 2$ (filled squares), $\text{Leu}^{98}\text{C}\delta 1$ (open circles), $\text{Ser}^{99}\text{N}^{\text{H}}$ (open uptriangles), $\text{Ala}^{103}\text{C}\beta$ (filled circles), $\text{Gly}^{110}\text{N}^{\text{H}}$ (open diamonds) and $\text{Glu}^{120}\text{N}^{\text{H}}$ (open downtriangles); and residues $\text{Asp}^{66}\text{N}^{\text{H}}$ (filled circles), $\text{Phe}^{67}\text{N}^{\text{H}}$ (filled squares), $\text{Thr}^{68}\text{N}^{\text{H}}$ (filled diamonds), $\text{Asn}^{71}\text{N}^{\text{H}}$ (filled uptriangle), $\text{Gly}^{74}\text{N}^{\text{H}}$ (open circles), $\text{Lys}^{76}\text{N}^{\text{H}}$ (open square), $\text{Ser}^{77}\text{N}^{\text{H}}$ (open uptriangle) and $\text{Lys}^{82}\text{N}^{\text{H}}$ (inset) are shown for groups I and II, respectively. **c, d**, Amides undergoing chemical exchange in free CypA and during turnover of the substrate *N*-succinyl-Ala-Phe-Pro-Phe-*p*-nitroanilide (green) are coloured in red and blue according to group I and II, respectively. All residues of group II are located in a loop region (blue). Dynamics of amides shown in grey could not be characterized because of the absence of the amide (Pro) or peak overlap. Dynamics data are plotted on the crystal structures of free CypA and CypA bound to the *cis* conformer of a similar substrate¹⁶, shown in two views (**c** and **d**) differing by a 90° horizontal rotation. **e**, Methyl side chains exhibiting chemical exchange during catalysis are shown in orange; those that do not show dispersion are shown in black. For each relaxation dispersion curve, two duplicate points were collected and used to estimate the absolute uncertainties together with the signal-to-noise ratio of each individual spectrum.

fitted with single rate constants is indicative of networks with collective motions, but it is not proof. As a direct test of the collective nature of the dynamics and to identify residues that build a common network, the system was locally disturbed by mutations within the network, and the effects of these mutations on the structure and dynamics were examined. We compared mutations in the active site—R55A, R55K and F113W—with amino-acid substitutions within loops adjacent to the active site, H70A and K82A (Fig. 2). These residues were chosen because they are located at different positions within the dynamic network. In addition, Lys 82 is drastically affected by substrate binding⁵ despite the fact that it is more than 10 Å from the substrate in the crystal structure¹⁶. Catalytic activities, given as k_{cat}/K_m (ref. 17), were severely diminished for the active-site mutants (R55A, $0.09 \pm 0.01\%$; R55K, $0.1 \pm 0.01\%$; F113W, $0.03 \pm 0.01\%$), whereas mutations in the loop did not markedly alter enzymatic activities (H70A, $108 \pm 10\%$; K82A, $88 \pm 7\%$). All mutants except H70A had lower substrate affinities, as determined from chemical-shift changes as a function of substrate concentration. Mutation of Arg 55 results in greatly decreased activity because this residue lowers the activation barrier of *cis-trans* isomerization by decreasing the double-bond character of the prolyl peptide bond through hydrogen bonding to the proline nitrogen.

All mutations cause chemical-shift changes, indicating changes in chemical environment that propagate throughout much of the protein. Moreover, it does not matter from which 'end' the system is disturbed; changes are always seen in a common network. By cross-correlating the chemical-shift changes caused by the mutations (Fig. 2d–f), we identified networks between sites. Remarkably, these networks are similar to those identified by conformational exchange on the wild-type enzyme (Fig. 1c–e).

What is the physical reason for this similarity? ^{15}N relaxation dispersion experiments on all mutants showed not only chemical exchange at a similar set of residues to those in the wild type but also similar exchange rates (k_{ex} ; Supplementary Table S1). However, the amplitudes of the dispersion profiles were changed by constant factors for nearly all amides for each mutant (Fig. 3a). This must reflect a shift in relative populations of the two exchanging states because k_{ex} remains the same (equation (1)). It also implies that the chemical shifts between the two states ($\Delta\omega$), and hence their structural differences, are identical for wild-type CypA and all CypA mutants (scheme (3)); Supplementary Table S2). Consequently, the dynamics data of the mutants provide direct evidence for the

collectiveness of motions and show that the mutations shift a highly skewed conformational equilibrium that is already present in wild-type CypA. Although most mutations such as H70A and K82A shift the equilibrium towards the minor state, R55A and binding of the inhibitor CsA have the opposite effect. In fact, the equilibrium is so far shifted towards the major conformation in the presence of CsA (more than 98%) that dispersion could be detected only for those amides with exceptionally large chemical-shift differences. A suppression of chemical exchange in CypA by CsA has previously been described qualitatively¹⁸. We now state the physical underpinning for this phenomenon: that inhibitor binding shifts a pre-existing equilibrium towards the major conformation. The observed global response to mutagenic perturbations further suggests that the dynamics of the loop region, although exhibiting a different exchange rate, is correlated with the dynamics of the core. Structurally this makes sense because Phe 67 within the loop region is part of a hydrophobic cluster that includes Leu 39, Phe 46, Phe 48 and Ile 78.

To corroborate the collective nature of the conformational transition, we performed an additional type of measurement on all amides. In this experiment, the sign of the changes in ^{15}N chemical shift between the major and minor states were determined for wild-type and mutant forms of CypA by measuring ^{15}N chemical-shift differences, Ω_N , between heteronuclear single-quantum coherence (HSQC) and heteronuclear multiple-quantum coherence (HMQC) spectra (Fig. 3b). Ω_N depends on the position in the ^{15}N dimension of the minor form with respect to the major form and on the relative populations¹⁹. For all amides with measurable differences, the signs are the same in all CypA forms. The amount of shift for all detected amides is proportional to the population differences determined from the relaxation dispersion experiments (Fig. 3c). This independent experiment further supports our original observation of collective dynamics in the free enzyme. Furthermore, ^{15}N chemical shifts of the minor conformation are not that of an unfolded protein²⁰, revealing the sampling of folded substrates.

We have thus shown that the conformational exchange in CypA detected during catalysis already exists in the absence of substrate. In other words, the enzyme's intrinsic dynamic 'personality' is well suited to its catalytic role. Moreover, the frequencies of these intrinsic motions are almost identical in the resting and turning-over enzyme and coincide with the overall turnover number. This correspondence might be of wide-ranging importance, given that in many enzymes, such as triosephosphate isomerase^{21,22}, dihydrofolate reductase^{23,24},

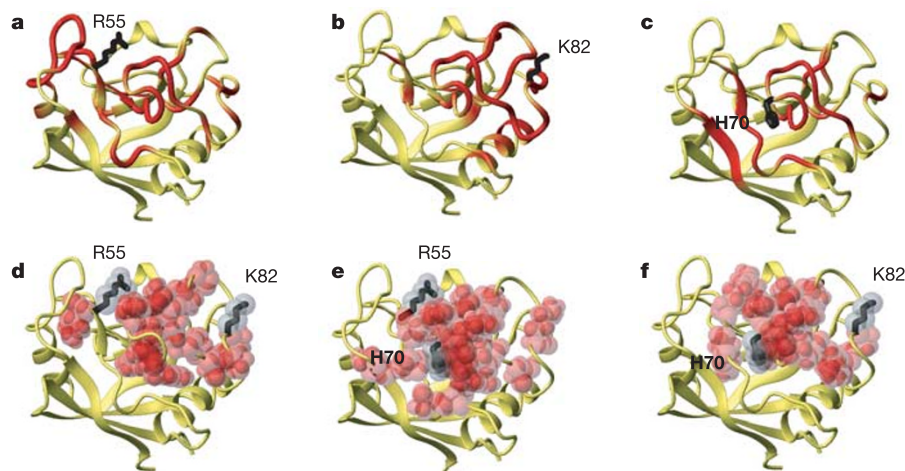


Figure 2 | Identification of residues that build a common dynamic network in CypA. **a–c**, Amide resonances for R55A (**a**), K82A (**b**) and H70A (**c**) that show changes in chemical shift relative to wild-type CypA are coloured in

red. **d–f**, Common residues with chemical-shift changes in R55A and K82A (**d**), R55A and H70A (**e**) and H70A and K82A (**f**) are displayed in red as van der Waals radii, delineating the collective network.

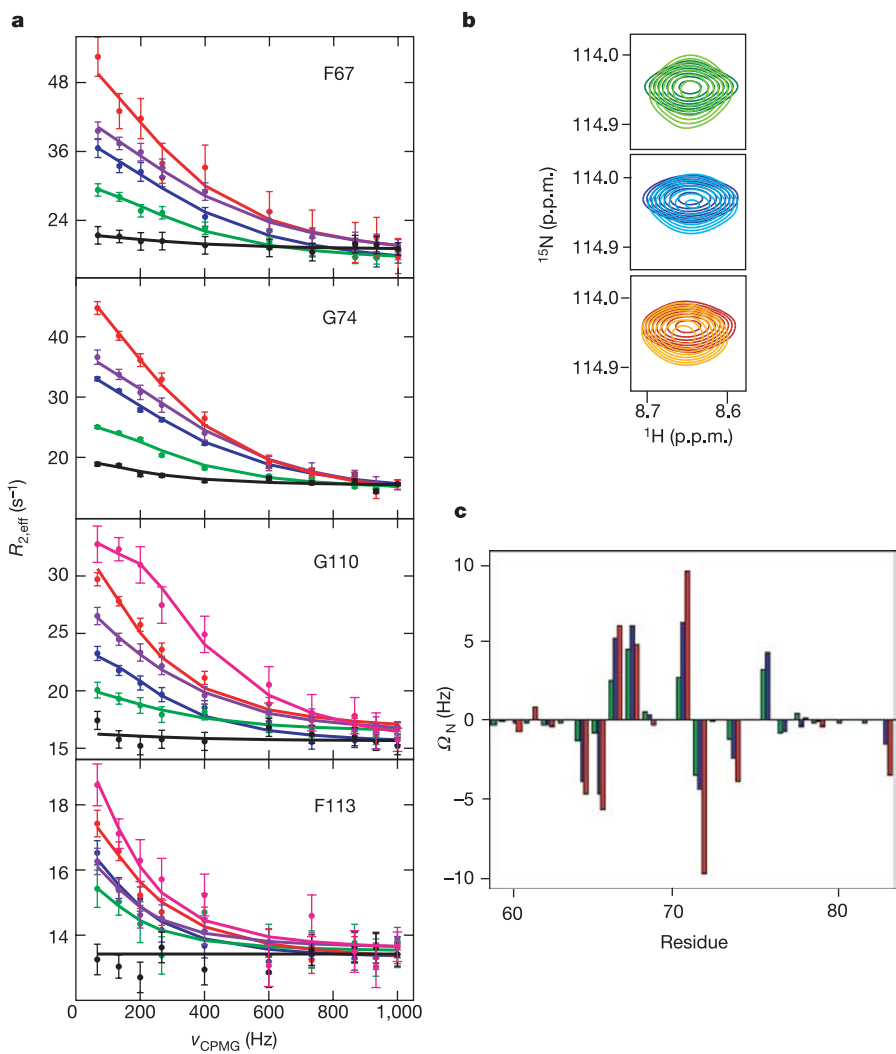


Figure 3 | Probing correlated motions of CypA by point mutations. **a**, CPMG relaxation dispersion data of four representative ^{15}N backbone amides are shown for the wild type (blue), R55K mutant (violet), R55A mutant (green), K82A mutant (red), H70A mutant (magenta) and wild-type CypA bound to CsA (black). Although the k_{ex} values for all forms are similar, the amplitudes of the dispersion profiles, which are proportional to R_{ex} , differ between the forms by a constant factor directly reflecting changes in populations of the two exchanging states. **b, c**, Mutations shift the populations of exchanging states as established by a comparison of chemical shifts of the major conformer in HSQC (darker colour) and HMQC (lighter colour) spectra¹⁹, visualized for Gly 74 in R55A (green), wild type (blue) and K82A (orange). **b**, The less populated state is shifted upfield in the ^{15}N dimension relative to the major conformation for all proteins tested. **c**, The differences in ^{15}N chemical shift between HSQC and HMQC spectra (Δ_N) (ref. 19) for residues 60–83 are shown for R55A (green), wild type (blue) and K82A (red). The relative changes in Δ_N between the different forms of CypA are proportional to the changes in population¹⁹ determined from the dispersion profiles in **a**. Error analysis was performed as described in the legend to Fig. 1.

HIV-1 protease²⁵, RNase A²⁶ and many others¹⁴, motions with rates of the same order of magnitude as the turnover number have been detected in their free or ligand-bound state. The similarity of dynamics in free and catalytically active CypA, together with these data on other enzymes, indicates that in enzymes with a fast turnover, catalytic power might be limited by rates of conformational rearrangements.

Our results provide further experimental evidence that the observed fluctuations at equilibrium are a result of a concerted global process. The identification of an extended dynamic network in CypA illustrates how proteins can propagate local changes over large distances. Coupled networks in proteins have previously been proposed on the basis of computational techniques^{3,7,8} and sequence-based methodologies⁹, and recent computational studies on CypA during substrate turnover have suggested correlated dynamic networks that largely agree with our experimental findings¹⁰.

Although the existence of motions in proteins is a fundamental thermodynamic concept, our results show pre-sampling of conformational substates before catalysis that are harvested for catalytic turnover. This is directly analogous to recent findings of the role of pre-existing equilibria for allosteric signalling and ligand binding^{14,27}. A picture is therefore emerging in which conformational events that occur during protein function are already present before ligands bind. In contrast to being folded in a single native conformation, proteins have evolved to sample multiple defined conformations that are critical for function. The concept of conformational substates and exploration of the energy landscape of proteins was put forward 30

years ago by Frauenfelder and collaborators⁶; the challenge now is to understand the connections between structure, energy landscapes, dynamics and function.

METHODS

Materials and enzyme activity. Wild-type and mutant proteins were expressed and purified as described previously⁵. For CypA containing [^{13}C]methyl-labelled CypA was produced as described previously²⁸.

Unless otherwise noted, NMR samples contained 0.7 mM CypA in 50 mM Na_2HPO_4 pH 6.5, and 1 mM dithiothreitol with 10% $^2\text{H}_2\text{O}$. The peptide *N*-succinyl-Ala-Phe-Pro-Phe-*p*-nitroanilide was used for NMR studies of CypA dynamics during catalysis and for activity assays by the coupled chymotrypsin assay at 10 °C (ref. 17). At least three measurements were used to determine k_{cat}/K_m values and their respective uncertainties. For saturated NMR samples 3.2 mM peptide and 3.5 mM CsA were used.

NMR spectroscopy and data analysis. All spectra were collected on Varian 600-MHz and 800-MHz spectrometers. Chemical shifts for CypA alone and in the presence of CsA were published previously¹⁸. Chemical shifts for CypA in the presence of substrate were determined with substrate titration data and confirmed by three-dimensional nuclear Overhauser enhancement spectroscopy–HSQC, a CBCA(CO)NH and a HNCACB spectrum (where CA is the alpha carbon and CB is the beta carbon).

Unless noted otherwise, all ^{15}N CPMG relaxation data were collected at 10 °C and 600 MHz. This lower temperature was used because of the much higher binding affinity for the substrate than at 25 °C (refs 5, 15). Data were collected on free CypA at 25 °C with protein concentrations of 1 and 2 mM to rule out sample aggregation effects on chemical exchange (Supplementary Fig. S1). Amide spectra were collected with TROSY (transverse relaxation-optimized spectroscopy)-CPMG sequences^{13,29}, applying 10–14 CPMG field strengths

ranging from 50 to 1,000 Hz. Methyl side-chain CPMG pulse sequences¹³ were performed at 10 °C at 600 and 800 MHz.

Relaxation dispersion data were based on peak intensities and analysed with the generalized Carver–Richard equation for a two-site exchange³⁰ with the use of in-house scripts. For each relaxation dispersion curve two duplicate points were collected and used to estimate the absolute uncertainties together with the signal-to-noise ratio of each individual spectrum. Dispersion curves were then fitted individually to a two-site exchange for all residues exhibiting chemical exchange.

For CypA in the presence of saturating substrate concentration, the individual fits gave exchange rates between 2,400 and 3,000 s⁻¹ justifying a global fit. For free CypA, individual fits clustered in two groups with rates in the ranges 900–1,400 s⁻¹ for group I and 2,000–3,000 s⁻¹ for group II. The separation of residues into these two groups was strongly buttressed by dispersion experiments at 25 °C, at which temperature the difference in rates between the two groups is more pronounced (Supplementary Fig. S2). Residues within those groups were fitted globally. Uncertainties for all global fits were calculated with a jackknife approach (Supplementary Table S1).

The similarity of exchange rates extracted from fits of dispersion profiles on a per-residue basis supports a two-state model of exchange. To establish further that this is true we compared a series of point mutants. Changes in global amplitude by constant factors in relaxation dispersion profiles for the mutant forms of CypA (Fig. 3a and Supplementary Table S3) with nearly identical exchange rates can be interpreted only by a shift in population between two states. Exact absolute populations cannot be determined because the process is in the fast exchange limit for most resonances and the chemical-shift difference is not known. However, data for the wild type and mutants can be fitted only with highly skewed populations (Supplementary Table S2). The observed k_{ex} and R_{ex} values define an upper limit of about 7% for the minor conformation of wild-type CypA because larger populations would yield $\Delta\omega$ values (equation (1)) that were so small as to result in unobservable chemical-shift changes in ¹⁵N HSQC experiments for the mutants. The result of highly skewed populations is further buttressed by simultaneous fits of [¹³C]methyl dispersion data at 600 and 800 MHz of residues with exchange in the intermediate time regime ($\alpha < 1.5$; ref. 14), for which p_{minor} was calculated to be 5%.

HMQC and HSQC spectra were collected at 10 °C and 600 MHz for wild-type and mutant forms of CypA with the use of recently published pulse sequences¹. Chemical shifts of the minor enzyme form ($\omega_{E_{\text{minor}}}$) were calculated by using $\Delta\omega$ obtained from the dispersion experiments (equation (1)) together with the sign of $\Delta\omega$ determined from the HMQC/HSQC experiment. Although the relation between the frequency differences of corresponding correlations in HMQC and HSQC data sets in the general case of an exchanging system is complex (see for example, equation (5) of ref. 19), simulations establish that the correlation between the difference and the population of the minor state, p_B , is nearly linear for $p_B \leq 0.15$. Thus, in an exchange involving highly skewed populations, the relative shifts of HMQC and HSQC correlations as a function of a perturbation that does not change the rate and shift differences between states can be used as a direct measure of changes in p_B .

Received 27 June; accepted 3 August 2005.

1. Jencks, W. P. *Catalysis in Chemistry and Enzymology* (Dover, New York, 1987).
2. Hammes, G. Multiple conformational changes in enzyme catalysis. *Biochemistry* **41**, 8221–8228 (2002).
3. Benkovic, S. J. & Hammes-Schiffer, S. A perspective on enzyme catalysis. *Science* **301**, 1196–1202 (2003).
4. Garcia-Viloca, M., Gao, J., Karplus, M. & Truhlar, D. G. How enzymes work: analysis by modern rate theory and computer simulations. *Science* **303**, 186–195 (2004).
5. Eisenmesser, E. Z., Akke, M., Bosco, D. A. & Kern, D. Enzyme dynamics during catalysis. *Science* **295**, 1520–1523 (2002).
6. Austin, R. H. et al. Dynamics of ligand binding to myoglobin. *Biochemistry* **14**, 5355–5373 (1975).
7. Berendsen, H. J. C. & Hayward, S. Collective protein dynamics in relation to function. *Curr. Opin. Struct. Biol.* **10**, 165–169 (2000).
8. Rod, T. H., Radkiewicz, J. L. & Brooks, C. L. Correlated motion and the effect of distal mutations in dihydrofolate reductase. *Proc. Natl. Acad. Sci. USA* **100**, 6980–6985 (2003).

9. Suel, G. M., Lockless, S. W., Wall, M. A. & Ranganathan, R. Evolutionarily conserved networks of residues mediate allosteric communication in proteins. *Nature Struct. Biol.* **10**, 59–69 (2003).
10. Agarwal, P. K., Geist, A. & Gorin, A. Protein dynamics and enzymatic catalysis: Investigating the peptidyl-prolyl cis-trans isomerization activity of cyclophilin A. *Biochemistry* **43**, 10605–10618 (2004).
11. Schmid, F. X. Prolyl isomerases. *Adv. Protein Chem.* **59**, 243–282 (2001).
12. Goff, S. P. Genetic control of retrovirus susceptibility in mammalian cells. *Annu. Rev. Genet.* **38**, 61–85 (2004).
13. Mulder, F. A. A., Mittermaier, A., Hon, B., Dahlquist, F. W. & Kay, L. E. Studying excited states of proteins by NMR spectroscopy. *Nature Struct. Biol.* **8**, 932–935 (2001).
14. Palmer, A. G. NMR characterization of the dynamics of biomacromolecules. *Chem. Rev.* **104**, 3623–3640 (2004).
15. Kern, D., Kern, G., Scherer, G., Fischer, G. & Drakenberg, T. Kinetic analysis of cyclophilin-catalyzed prolyl cis/trans isomerization by dynamic NMR spectroscopy. *Biochemistry* **34**, 13594–13602 (1995).
16. Zhao, Y. & Ke, H. Crystal structure implies that cyclophilin predominantly catalyzes the trans to cis isomerization. *Biochemistry* **35**, 7356–7361 (1996).
17. Fischer, G., Bang, H. & Mech, C. Determination of enzymatic catalysis for the cis-trans-isomerization of peptide binding in proline-containing peptides. *Biochem. Biophys. Acta* **43**, 1101–1111 (1984).
18. Ottiger, M., Zerbe, O., Guntert, P. & Wuthrich, K. The NMR solution conformation of unligated human cyclophilin A. *J. Mol. Biol.* **272**, 64–81 (1997).
19. Skrynnikov, N. R., Dahlquist, F. W. & Kay, L. E. Reconstructing NMR spectra of ‘invisible’ excited protein states using HMQC and HMQC experiments. *J. Am. Chem. Soc.* **124**, 12352–12360 (2002).
20. Wishart, D. S., Sykes, B. D. & Richards, F. M. Relationship between nuclear magnetic resonance chemical shift and protein secondary structure. *J. Mol. Biol.* **222**, 311–333 (1991).
21. Rozovsky, S., Jogi, G., Tong, L. & McKermott, A. E. Solution-state NMR investigations of triosephosphate isomerase active site loop motion: ligand release in relation to active site loop dynamics. *J. Mol. Biol.* **310**, 271–280 (2001).
22. Williams, J. C. & McDermott, A. E. Dynamics of the flexible loop of triosephosphate isomerase: the loop motion is not ligand gated. *Biochemistry* **34**, 8309–8319 (1995).
23. Schnell, J. R., Dyson, H. J. & Wright, P. E. Structure, dynamics, and catalytic function of dihydrofolate reductase. *Annu. Rev. Biophys. Biomol. Struct.* **33**, 119–140 (2004).
24. McElheny, D., Schnell, J. R., Lansing, J. C., Dyson, H. J. & Wright, P. E. Defining the role of active-site loop fluctuations in dihydrofolate reductase catalysis. *Proc. Natl. Acad. Sci. USA* **102**, 5032–5037 (2005).
25. Ishima, R., Freedberg, D. I., Wang, Y. X., Louis, J. M. & Torchia, D. A. Flap opening and dimer-interface flexibility in the free and inhibitor-bound HIV protease, and their implications for function. *Struct. Fold. Des.* **7**, 1047–1055 (1999).
26. Cole, R. & Loria, J. P. Evidence for flexibility in the function of ribonuclease A. *Biochemistry* **41**, 6072–6081 (2002).
27. Volkman, B. F., Lipson, D., Wemmer, D. E. & Kern, D. Two-state allosteric behaviour in a single-domain signalling protein. *Science* **291**, 2429–2433 (2001).
28. Rosen, M. K. et al. Selective methyl group protonation of perdeuterated proteins. *J. Mol. Biol.* **263**, 627–636 (1996).
29. Loria, J. P., Rance, M. & Palmer, A. G. A TROSY CPMG sequence for characterizing chemical exchange in large proteins. *J. Biomol. NMR* **15**, 151–155 (1999).
30. Carver, J. P. & Richards, R. E. A general two-site solution for the chemical exchange produced dependence of T2 upon the Carr–Purcell pulse separation. *J. Magn. Reson.* **6**, 89–105 (1972).

Supplementary Information is linked to the online version of the paper at www.nature.com/nature.

Acknowledgements We thank K. H. Wildman for discussions. This work was supported by NIH grants to D.K., by a grant from the Canadian Institutes of Health Research to L.E.K., and by a grant from the Swedish Research Council to M.W.W. Part of the NMR studies was performed at the NHMFL at Florida with support from the NSF.

Author Information Reprints and permissions information is available at npg.nature.com/reprintsandpermissions. The authors declare no competing financial interests. Correspondence and requests for materials should be addressed to D.K. (dkern@brandeis.edu).